FRACTURE DYNAMICS OF A PROPAGATING CRACK IN A PRESSURIZED DUCTILE CYLINDER

A. F. EMERY, W. J. LOVE, A. S. KOBAYASHI

Department of Mechanical Engineering,
University of Washington, Seattle, Washington 98195, U.S.A.

SUMMARY

A suddenly-introduced axial through-crack in the wall of a pipe pressurized by hot water is allowed to propagate according to Weiss' notch-strength theory of ductile static fracture. For this somewhat ductile material of A533B steel, Weiss' criterion, which was extended to dynamic fracture without modification, fracture occurs when the dynamic circumferential-strain, $\varepsilon_{\theta\theta}$, at a distance of $r_p = K_{IC}^2/\pi\sigma_{ys}$ ahead of the moving crack tip is equal to the yield-strain of the material. This dynamic-fracture criterion enabled us to obtain a unique comparison of the results of ductile-fracture with those of brittle-fracture in a fracturing A533B steel pipe. Since the pipe cross-sectional area is likely to increase with large flap motions under ductile tearing, a large deformation-shell-finite-difference-dynamic-code which includes rotary inertia was used in this analysis. The uniaxial-stress-strain curve of A533B steel was approximated by a bilinear stress-strain where Von-Misses yield criterion and associated flow rule were used in the elastic-plastic analysis. The fluid pressure was assumed constant and thus pipe flaps are only lightly loaded by pressure in this analysis. In previous publications, the authors have compared their preliminary results for the shell motion obtained through their model for a fracturing pipe with those of Kanninen, *et al.*, and Freund, *et al.*, to evaluate the effects of pressure loading on the crack flaps and the differences between small and large deflection results. In this paper, we discuss the differences in crack-propagation behavior of a fracturing pipe composed of the same A533B but subjected to a brittle or a ductile-fracture criterion.

The fracture toughness of A533B steel was assumed to be 60 ksi $\sqrt{\text{in.}}$ and uniaxial-yield strain was assumed to be $\varepsilon_{ys} = 0.002569$ which was prescribed at $r_p = .1053$ in. ahead of the crack tip. Two internal-pressure-loadings of $p = 200$ and 500 psi were considered. As expected, crack propagation initiated about 10 microseconds earlier in both the brittle and the ductile pipes at the higher pressure loading of 500 psi. Crack velocities for the low-pressure varied intermittently with distinct periods of apparent crack-arrest or delay appearing after the crack had approximately doubled its initial length. This intermittent-crack-propagation phenomenon was less distinct in ductile pipes and high-pressure pipes. Similar intermittent-crack propagations have been predicted in the Kanninen model of wedge-loaded DCB specimen and to a lesser extent in the extensive experimental data published by Hahn, *et al.*, on the wedge-loaded DCB model and the tapered-DCB-specimen by Ripling, *et al.* In interpreting the crack-velocity data the latter investigators ignored the existence of the small fluctuations and this procedure in data analysis was modeled numerically by driving the crack with crack velocities obtained by a smooth-fitting of the crack velocities obtained from the calculations based on a constant dynamic fracture criterion. The K_{ID} and ε_{ys} determined from the low- and high-pressure calculations oscillated with variation noted for the high-pressure case. An important conclusion in fracture dynamics derived from these analyses is that a smoothly-varying crack velocity will require a non-unique crack-velocity-versus-dynamic-fracture-parameter-relation while a unique and smoothly-varying crack-velocity-versus-dynamic-fracture-parameter-relation will demand an intermittently-propagating crack.

1. Introduction

Dynamic fracture of pressurized pipes depends upon the structural response of the pipe to the precise mode of fracture and upon the pressure distribution within the pipe and on the opening flaps of the crack. The crack propagation history must be estimated through the simultaneous calculation of the fluid pressure, which is influenced by the cross sectional shape of the pipe, and the dynamic deflections of the pipe, which are influenced by the changing pressures due to fluid loss through the crack opening. Furthermore, the fluid pressure reflections from a reservoir can raise the pipe pressure and force a continued crack extension even though the fluid outflow may tend to cause crack arrest [1]. Consequently the study of the dynamic crack extension of the pressurized pipe requires an interactive analysis and as such effectively precludes an efficient numerical study of the crack tip extension. If we can establish that the fluid and structural problems are separable, then the study will be more facile.

In previous papers, Emery et al. reported elastic [2] and plastic deformations of fracturing pipes using constant pressure, and coupled pressure-deformation calculations [3,4]. These calculations were conducted for hot water pressurized pipes in which the initial outflow through the crack produced an immediate single phase depressurization to the fluid saturation pressure and a consequent light loading of the flaps. In a sequel paper, Emery et al. analyzed ductile tearing of an air-filled pipe in which the pressure downstream of the crack tip decayed slowly [5]. This analysis, which is in agreement with Freund [6], showed that the pressure distributions on the flaps did not appreciably affect the crack velocity and that the dynamic motion of the flaps could be modeled by Kanninen's simpler and more qualitative model [7]. By using such a simplified model for gases at crack velocities below or in the vicinity of the fluid sonic values, and noting that the axial crack propagation can be predicted by a constant pressure distribution which moves with the crack tip, it was concluded that the gas pressure analysis could be carried out independently of the structural analysis. Emery et al. [8] used these assumptions in their study of the effects of differences in dynamic fracture toughness upon the crack propagation history. In that study, they showed that a smoothly varying or constant stress intensity factor led to an intermittent crack motion, while a smooth crack motion required a rapidly varying dynamic fracture toughness. Here we wish to determine if these conclusions are valid for ductile fractures.

2. Structural Analysis

2.1 Basic Equations

Consider a cylindrical shell of thickness 2h and midsurface radius a as shown in Figure 1. By defining u and v as the midsurface deflections in the x and θ directions, respectively, w the radial deflection, and α and β as the midsurface rotations, the dynamic equations of motion with the assumptions of plane sections remaining plane and of small strains but large deformations are

$$A\ddot{u} + B\ddot{\alpha} = a\frac{\partial \bar{N}_{11}}{\partial x} + \frac{\partial \bar{N}_{21}}{\partial \theta} + a\bar{T}_1^N \tag{1a}$$

$$B\ddot{u} + C\ddot{\alpha} = a\frac{\partial \bar{M}_{11}}{\partial x} + \frac{\partial \bar{M}_{21}}{\partial \theta} + ah\bar{T}_1^M - a\bar{Q}_1$$

$$(A + \frac{B}{a})\ddot{v} + B\ddot{\beta} = a\frac{\partial \bar{N}_{12}}{\partial x} + \frac{\partial \bar{N}_{22}}{\partial \theta} + a\bar{T}_2^N + \bar{Q}_2 \tag{1c}$$

$$(B + \frac{C}{a})\ddot{v} + C\ddot{\beta} = a\frac{\partial \overline{M}_{12}}{\partial x} + \frac{\partial \overline{M}_{22}}{\partial \theta} + a\overline{T}_2^M - a\overline{Q}_2 \tag{1d}$$

$$A\ddot{w} = a\frac{\partial \overline{Q}_1}{\partial x} + \frac{\partial \overline{Q}_2}{\partial \theta} - \overline{N}_{22} + a\overline{T}_3 \tag{1e}$$

where

$$\{A,\ B,\ C\} = \int_{-h}^{h} \rho r\ \{1,\ z,\ z^2\}dz \tag{1f}$$

The rotations α and β are different from the rotations $-\frac{\partial w}{\partial x}$ and $-\frac{1}{r}\frac{\partial w}{\partial \theta}$ of lines which were originally normal to the midsurface, and relate to transverse shear and to rotatory inertia which are considered in this analysis. Because the axial crack has an opening mode in which the edges peel back, the effects of transverse shear and rotatory inertia are of substantial importance. The force and moment resultant N, M, AND Q and the surface tractions, T, for large deflections are defined in terms of the displacements, u, v and w, the rotations α, β, and the force and moment resultants for small deflections and are fully described in Reference [9]. The stresses during plastic deformations are computed by using the von-Mises yield criterion and the incremental plastic strain theory.

2.2 Finite Different Algorithm for Shell

The shell is subdivided into a series of nodal points by the mesh illustrated in Figure 2 with the force and moment resultants defined at the appropriate points as indicated. Special care must be taken to ensure second order accuracy at every mesh point in order to prevent anomalous effects such as "keystoning" and large gaps in the frequency spectrum of the algorithm [10]. By using an explicit-formulation the equations can be solved directly for the displacements and rotations at time t + Δt without a matrix inversion, subject only to the time step stability restrictions of

$$C_o\Delta t < 2h,\quad C_o^2 = \frac{E}{\rho(1 - \nu^2)} \tag{6a}$$

$$2h < \frac{a\Delta x\Delta\theta}{\sqrt{\Delta x^2 + a^2\Delta\theta^2}} \tag{6b}$$

The first requirement is based upon the need for an accurate calculation of the shear deformation mode and is especially restrictive when compared to the usual criterion of shell analysis. Since the purpose of the calculation is to determine the shearing deformation of the crack edges, however, such small time steps are a necessity. The second criterion simply required that the shell thickness be less than the mesh width and is a natural requirement in shell analysis.

3. Dynamic Fracture of a Steel Pipe

A steel cylindrical shell with an internal radius of R = 3 inches and cylindrical wall thickness of h/a = 1/30, was divided into a finite difference mesh of $\Delta\theta$ = 9° and $\Delta x/a\Delta\theta$ = 1/2. The shell was taken to be three radii long with the outgoing wave boundary condition imposed at the fluid supply end of the cylinder. The cylinder was assumed to be composed of A533B steel with a constant fracture toughness of 60 ksi$\sqrt{\text{in}}$ (65.4 MPa$\sqrt{\text{m}}$).

As a mechanism of initiating crack propagation, initial crack surfaces were first closed and the shell was given a deflection w^o correspoding to a constant internal pressure P_o. At time zero, the two crack surfaces were released and the resultant dynamic motion was calculated. Figure 3 shows the change in the hoop stress resultant, N_{22}, at half nodal distance,

$\Delta x/2$, ahead of the crack when the crack tip was not permitted to move. The reflection of the stress wave, produced by the crack opening, from the plane of symmetry (at 180° from the crack surface) is clearly seen near the time of 100 microseconds. The crack was then subjected to a criterion for onset of crack propagation. For A533B steel, which is somewhat ductile, Weiss' [11] notch-strength theory of ductile static fracture was extended to dynamic fracture without modification. According to this criterion, fracture occurs when the dynamic circumferential strain, $\varepsilon_{\theta\theta}$, at a distance of $r_p = K_{IC}^2/2\pi\sigma_{ys}^2$ ahead of the moving crack tip is equal to the yield-strain of the material. For these calculations the uniaxial-yield strain was assumed to be $\varepsilon_{ys} = 0.002569$ which was prescribed at a distance of $r_p = 0.1053$ in (0.00267 m) ahead of the crack tip. By using this criterion, it is possible to obtain a direct comparison with the brittle fracture studies [8] in which the fracture was presumed to occur when

$$N_{22} = \frac{K_D 2h}{\sqrt{2\,\frac{\Delta x}{2}}} \quad \text{as compared to} \quad \varepsilon_{\theta\theta} = \frac{\varepsilon_{ys}}{\Delta x/2}\,\frac{K_D^2}{2\pi\sigma_{ys}^2} \quad \text{for the ductile case.}$$

To illustrate both slow and fast cracks, the fluid pressures of 500 psi (3.448 MPa) and 200 psi (1.517 MPa) were used and as indicated on Figure 3, the high pressure caused a rapid initiation of crack extension while the low pressure barely achieved crack extension. The moderate ductility of this material, as evidenced by the proximity of the ductile and brittle onsets of fracture as shown in Figure 3, would lead us to assume that the dynamic behavior of the brittle and ductile fractures would be similar, although as we shall see later they are quite disparate.

Figure 4 shows the crack tip position versus time for the low internal pressures. The ductile crack tip velocities are approximately equal to those for the brittle fracture after the tip has moved a reasonable distance, but the intermittency is much more pronounced. The long periods of very slow motion are due to the pressure which is almost too low to initiate crack extension and also due to the tendency of the crack to outrun the opening force. Thus a long delay is necessary to reinitiate the extension. A slightly higher pressure produces a crack tip position history which is more similar to the brittle fracture history, but which still shows significant delays at early times. Figure 5 illustrates the crack tip history for the high pressure. Again the velocities are comparable, but now we see that the ductile case has a very smooth crack position versus time relation, albeit a delayed one, while the brittle case shows the intermittency to be very strong. Such intermittent crack motion has been reported by Kanninen et al. [7], for the past several years and is believed to result from the dynamic fracture toughness versus crack velocity relations assumed in the theoretical dynamic fracture criterion. Careful observation of the experimental data on dynamic crack tip motion versus time tends to verify the existence of such intermittent motions [12]. The general tendency, however, is to fit a smooth curve through the experimental data and thus produce a continuously varying crack velocity relation. Figure 6 shows the crack velocities measured for the low pressure ductile fracture and the smoothed crack velocity profile. Whereas the brittle fracture showed relatively constant velocities in the two distinct stages of motion, and thus was modeled by a constant velocity as indicated on Figure 6, the ductile case exhibited continously increasing high and low velocities (Figure 5) and the smooth velocity showed a continuous rise over the period of interest. The stress intensity factor was then computed by eq. (7) using the calculated circumferential strain. The results are plotted in

Figure 7, with the comparable brittle fracture results.

In contrast with the brittle calculations, where large and rapid oscillations in K_D are found, the ductile calculations are very close to the constant value, although some oscillations are still present. The standard deviation of the brittle case is 20% while that for the ductile case is only 7% with most of the error arising during the later stages of crack extension when the crack velocity is the highest. It should be noted that brittle and ductile cases converage to same values at longer crack length. It is interesting to observe that during the early stages when the velocity is most different from the smoothed values, the calculated K_D's are quite close to the original constant value.

Figure 8 shows the crack opening displacements for the propagating crack at several half-crack lengths, when propagating at constant K_D or at the smoothed velocity. Both cases show slight undulations whose origin is not yet clear. In the brittle calculations, the use of a constant K_D gave rise to opening displacements which always were slightly greater than those calculated for the smoothed velocity. The ductile case, however, showed significantly larger displacements and an intermediate reversal (for $x/L_{initial} = 1.62$). This was caused by the very high velocity present at this point in the constant K_D calculations. On the other hand, even for similar velocity disparities, the brittle calculations never displayed such a reversal of the trend. Both the brittle and the ductile opening displacements for all cases become essentially indistinguishable when plotted in the form u_2/u_{2max}, which suggests that the crack propagation characteristics are relatively insensitive to the dynamic fracture criterion.

4. Conclusions

A finite difference code with large deflection formulation was used to study the dynamic response of a running axial crack in a cylinder with constant pressure. The results of this analysis show that either: (a) the crack must run at intermittent crack velocities in order that a smoothly varying dynamic fracture toughness versus crack velocity relation exists as a material property, or (b) that the dynamic fracture toughness must vary in order to maintain smoothly varying and uniform crack velocities. However, these effects were found to be significantly less for the ductile fracture than for the brittle fracture and it may be impossible to experimentally observe these effects for the ductile crack propagation.

5. Acknowledgement

The work reported in this paper is sponsored by the Electric Power Research Institute under Contract RP231-1. The authors wish to thank Drs. J. Carey and C. Chan of EPRI for their encouragement through the course of this research program.

6. Nomenclature

a	Average radius of shell
C_1, C_2	Dilatational and shear wave velocities
h	Half thickness of shell
i,j	Mesh coordinates
M	Moment resultants
N	Force resultants
P	Pressure
Q	Shear resultants

r	Radial distance
t	Time
T	Surface loads
u,v,w	Axial, circumferential and radial displacements, respectively
x,z	Axial and thickness coordinates, respectively
α,β	Axial and circumferential rotations, respectively
θ	Angular coordinate
$\varepsilon_{i,j}$	Strains
ρ	Density

References

[1] SHOEMAKER, A.K., MCCARTNEY, R.F., "Displacement Consideration for a Ductile Propagating Fracture in a Line Pipe," J. of Engineering Material Technology, Trans. of ASME, 96, 318-322 (1974).

[2] EMERY, A.F., LOVE, W.J., KOBAYASHI, A.S., "Elastic Crack Propagation Along a Pressurized Pipe," J. of Pressure Vessel Technology, Trans. of ASME, 98, 2-8 (February 1976).

[3] EMERY, A.F., LOVE, W.J., KOBAYASHI, A.S., "Fracture in Straight Pipes Under Large Deflection Conditions - Part I, Structural Deformations," J. of Pressure Vessel Technology, Trans. of ASME, 99, Series J, No. 1, 122-127 (February 1977).

[4] LOVE, W.J., EMERY, A.F., KOBAYASHI, A.S., "Fracture in Straight Pipes Under Large Deflection Conditions - Part II, Pipe Pressures," ibid loc cit, 128-136.

[5] EMERY, A.F., LOVE, W.J., KOBAYASHI, A.S., "Dynamic Finite Difference Analysis of an Axially Cracked Pressurized Pipe Undergoing Large Deformation," to be published in Fast Fracture and Crack Arrest, ASTM STP 627 (1977).

[6] FREUND, L.B., PARKS, D.M., RICE, J.R., "Running Ductile Fracture in a Pressurized Line Pipe," Mechanics of Crack Growth, ASTM STP 590, 243-262 (1976).

[7] KANNINEN, M.F., SAMPATH, S.G., POPELAR, C., "Steady-State Crack Propagation in Pressurized Pipelines Without Backfill," J. of Pressure Vessel Technology, Trans. of ASME, 98, Series J, 56-65 (February 1976).

[8] EMERY, A.F., LOVE, W.J., KOBAYASHI, A.S., "Influence of Dynamic Fracture Toughess on Elastic Crack Propagation on a Pressurized Pipe," to be published in the Proc. of Int. Conf. on Fracture Mechanics and Technology, Hong Kong, March 21-25, 1977.

[9] EMERY, A.F., CUPPS, F.J., "RIBSTEAK: A Computer Program for Calculating the Dynamic Motion of Cylindrical and Conical Shells," Sandia Laboratory Report SLL 197.

[10] EMERY, A.F., CUPPS, F.J., "Finite Difference Computation of the Dynamic Motion of Cylindrical Shells Including the Effect of Rotatory Inertia and Transverse Shear," to be published in Earthquake Engineering and Structural Dynamics.

[11] WEISS, V., SENGUPTA, M., "Ductility, Fracture Resistance, and R-Curves," Mechanics of Crack Growth, ASTM STP 590, 194-207 (1977).

[12] HAHN, G.T., BEHLEN, R.C., HOAGLAND, R.G., KANNINEN, M.F., POPELAR, G., ROSENFIELD, A.R., DECAMPOS, V.S., "Critical Experiments, Measurements and Analysis to Establish a Crack Arrest Methodology for Nuclear Pressure Vessel Steels," Battelle Columbus Laboratories, BMI-1937 (August 1975).

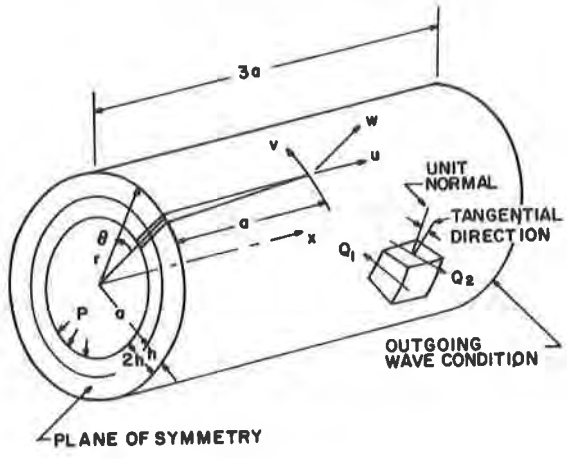

Figure 1. Fracturing Cylindrical Shell

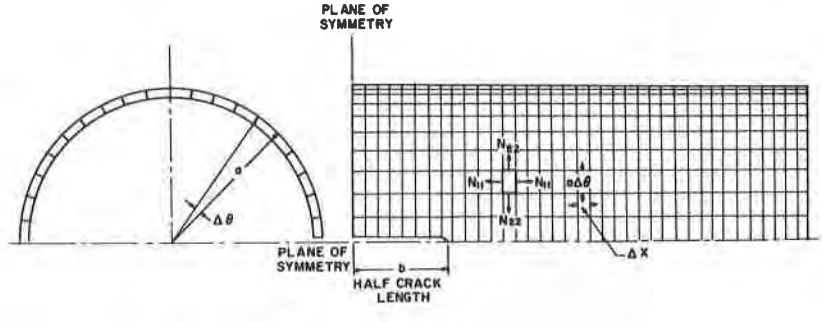

Figure 2. Finite Difference Mesh

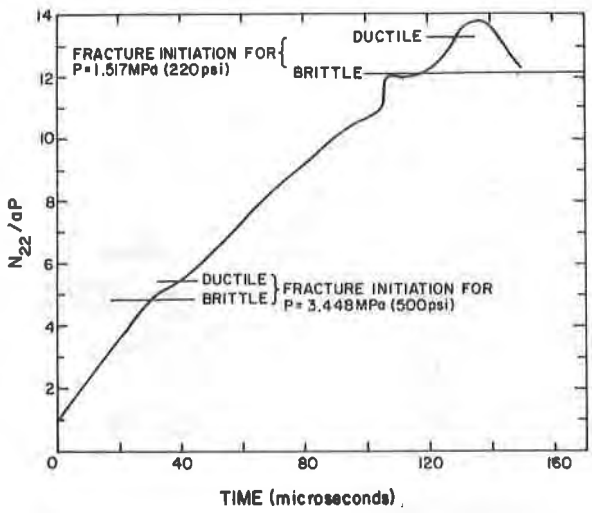

Figure 3. Stress Resultant N_{22} Measured at $\Delta x/2$ Ahead of the Crack Tip for a Fixed Crack Length. A533B Material

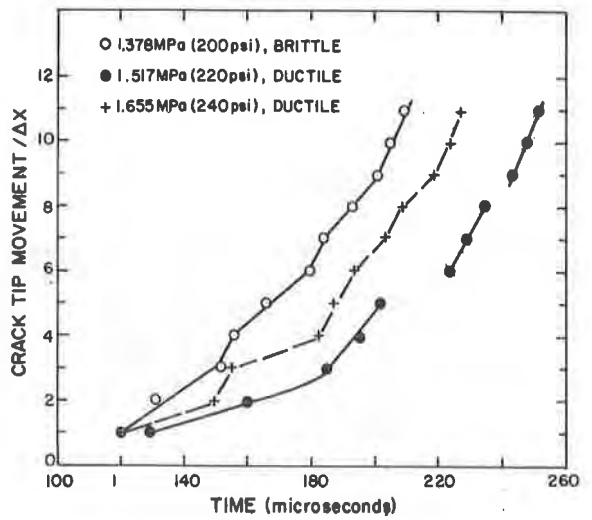

Figure 4. Crack Tip Movement for Several Low Internal Pressures

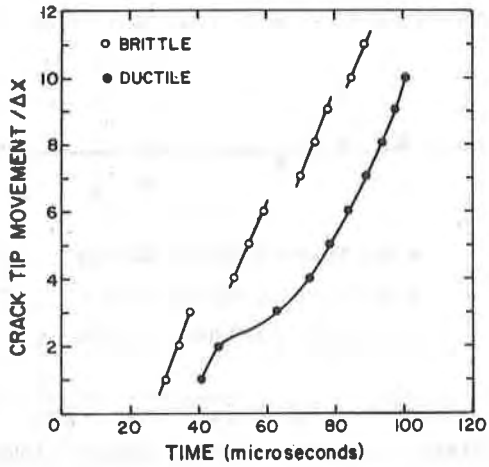

Figure 5. Crack Tip Movement for an Internal Pressure of 3.474 MPa (500 psi)

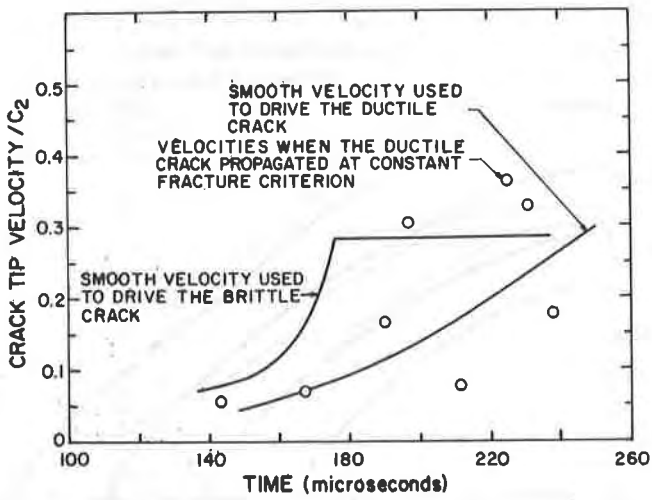

Figure 6. Crack Tip Velocities for an Internal Pressure at 1.517 MPa (220 psi)

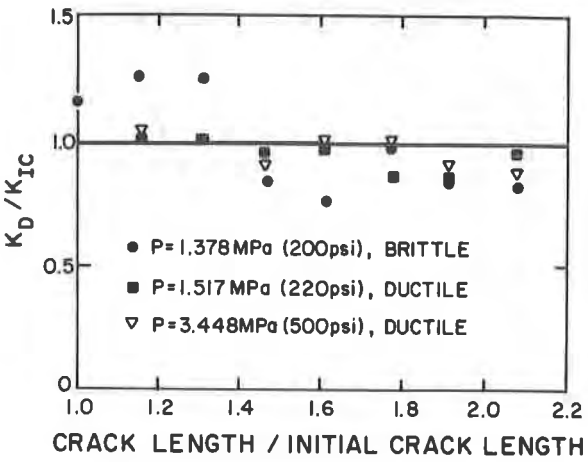

Figure 7. Stress Intensity Factor Calculated Δx/2 Ahead of the Tip for a Crack Driven with a Smooth Velocity Profile

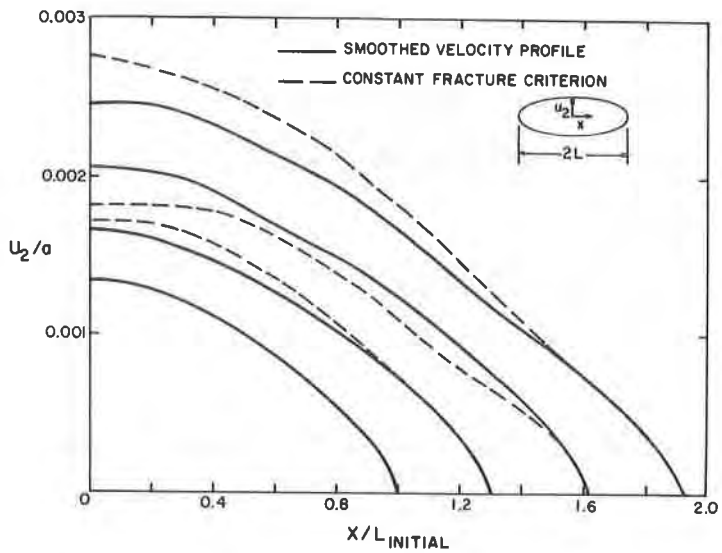

Figure 8. Crack Opening Displacements for an Internal Pressure of 1.517 MPa (200 psi)